

Multifractality of Inverse Statistics of Exit Distances in 3D Fully Developed Turbulence

Wei-Xing Zhou,^{1,2,*} Didier Sornette,^{2,3,4,†} and Wei-Kang Yuan^{1,‡}

¹*State Key Laboratory of Chemical Reaction Engineering,
East China University of Science and Technology, Shanghai 200237, China*

²*Institute of Geophysics and Planetary Physics,
University of California, Los Angeles, CA 90095*

³*Department of Earth and Space Sciences,
University of California, Los Angeles, CA 90095*

⁴*Laboratoire de Physique de la Matière Condensée,
CNRS UMR 6622 and Université de Nice-Sophia Antipolis, 06108 Nice Cedex 2, France*

(Dated: June 14, 2021)

Abstract

The inverse structure functions of exit distances have been introduced as a novel diagnostic of turbulence which emphasizes the more laminar regions [1, 2, 3, 4]. Using Taylor's frozen field hypothesis, we investigate the statistical properties of the exit distances of empirical 3D fully developed turbulence. We find that the probability density functions of exit distances at different velocity thresholds can be approximated by stretched exponentials with exponents varying with the velocity thresholds below a critical threshold. We show that the inverse structure functions exhibit clear extended self-similarity (ESS). The ESS exponents $\xi(p, 2)$ for small p ($p < 3.5$) are well captured by the prediction of $\xi(p, 2) = p/2$ obtained by assuming a universal distribution of the exit distances, while the observed deviations for large p 's characterize the dependence of these distributions on the velocity thresholds. By applying a box-counting multifractal analysis of the natural measure constructed on the time series of exit distances, we demonstrate the existence of a genuine multifractality, endowed in addition with negative dimensions. Performing the same analysis of reshuffled time series with otherwise identical statistical properties for which multifractality is absent, we show that multifractality can be traced back to non-trivial dependence in the time series of exit times, suggesting a non-trivial organization of weakly-turbulent regions.

PACS numbers: 47.53.+n, 05.45.Df, 02.50.Fz

*Electronic address: wxzhou@moho.ess.ucla.edu

†Electronic address: sornette@moho.ess.ucla.edu

‡Electronic address: wkyuan@ecust.edu.cn

I. INTRODUCTION

In isotropic turbulence, structure functions are among the favorite statistical indicators of intermittency. The (longitudinal) structure function of order p is defined by $S_p(r) \equiv \langle \delta v_{\parallel}(r)^p \rangle$. The K41 theory [5] obtains that $S_p(r) = C_p \epsilon^{p/3} r^{p/3}$, where ϵ is the average energy dissipation rate of the fluid element of size r and C_p is a constant independent of Reynolds number. The K62 theory [6] extends K41 by assuming a log-normal distribution of ϵ , which was questioned by Mandelbrot [7]. The anomalous scaling properties was uncovered experimentally [8] implying the non-Gaussianity of the probability distribution of the velocity increments.

The velocity structure functions consider the moments of velocity increments over space. However, when one turns to the scalar statistics in passive scalar advection, one often considers averages of the advection time versus the distance [9, 10]. An alternative quantity was introduced, denoted the distance structure functions [1] or inverse structure functions [3, 11]:

$$T_p(\delta v) \equiv \langle r^p(\delta v) \rangle, \quad (1)$$

where δv are a set of pre-chosen thresholds of velocity increments and $r(\delta v)$ is the *exit distance* defined as the minimal distance for the velocity difference to exceed δv

$$r(\delta v) = \inf \{ r : |v_{i\pm r} - v_i| > \delta v \} , \quad (2)$$

given a record of velocity v_i . In the literature, alternative definitions are adopted as well, such as $|v_{i+r} - v_i| > \delta v$ or $v_{i+r} - v_i > \delta v$.

To ensure that the exit distance is defined, the threshold δv should be less than $\delta v_{\max} = (v_{\max} - v_{\min})/2$, where v_{\max} and v_{\min} are respectively the maximum and minimum of the record. On the other hand, there is a minimal velocity increment $\delta v_{\min} = \min(|v_{i+1} - v_i|)$ for a given record such that for any $\delta v \leq \delta v_{\min}$ we have $r = 1$. Therefore, we consider the range $(\delta v_{\min}, \delta v_{\max})$. For any δv in this range, by construction, we will obtain finite r values from the velocity record.

The statistical properties studied for synthetic data of 24630 situations from the GOY shell model of turbulence exhibit perfect scaling dependence of the inverse structure functions on the velocity threshold [1]. A completely different result was obtained in [11] where an experimental signal was analyzed and no clear scaling was found in the exit distance structure

functions. For smoother stochastic fluctuations associated with a spectrum with exponent $3 \leq \beta < 5$, such as two-dimensional turbulence, the inverse structure functions exhibit bifractality [3]. While the large δv 's at fixed r of the velocity structure functions emphasize the most intermittent region in turbulence, the large r 's at fixed δv probe the laminar regions. Hence, the inverse structure functions provide probes of the intermediate dissipation range (IDR) [11] introduced in [12]. It is clear that the extreme events in the distribution of r provide the prevailing contributions to the inverse structure functions for large exponents, which should thus be investigated carefully.

To our knowledge, inverse structure functions (or equivalently the statistics of exit distances) have not been used to characterize experimental three-dimensional turbulence data. Here, we describe in detail the probability distribution of exit distances r and find that the stretched exponential distribution is a good approximation for all r 's. Then, we analyze the convergence of the inverse structure functions and investigate their multiscaling properties. We construct a measure based on the exit distance at each level δv and unveil the multifractal nature of the measure.

II. STANDARD PRELIMINARY TESTS ON THE EXPERIMENTAL DATA

Very good quality high-Reynolds turbulence data have been collected at the S1 ONERA wind tunnel by the Grenoble group from LEGI [8]. We use the longitudinal velocity data obtained from this group. The size of the velocity time series we analyzed is $N \approx 1.73 \times 10^7$.

The mean velocity of the flow is approximately $\langle v \rangle = 20\text{m/s}$ (compressive effects are thus negligible). The root-mean-square velocity fluctuations is $v_{\text{rms}} = 1.7\text{m/s}$, leading to a turbulence intensity equal to $I = v_{\text{rms}}/\langle v \rangle = 0.0826$. This is sufficiently small to allow for the use of Taylor's frozen flow hypothesis. The integral scale is approximately 4m but is difficult to estimate precisely as the turbulent flow is neither isotropic nor homogeneous at these large scales.

The Kolmogorov microscale η is given by [13] $\eta = \left[\frac{\nu^2 \langle v \rangle^2}{15 \langle (\partial v / \partial t)^2 \rangle} \right]^{1/4} = 0.195\text{mm}$, where $\nu = 1.5 \times 10^{-5} \text{m}^2 \text{s}^{-1}$ is the kinematic viscosity of air. $\partial v / \partial t$ is evaluated by its discrete approximation with a time step increment $\partial t = 3.5466 \times 10^{-5} \text{s}$ corresponding to the spatial resolution $\delta_r = 0.72\text{mm}$ divided by $\langle v \rangle$.

The Taylor scale is given by [13] $\lambda = \frac{\langle v \rangle v_{\text{rms}}}{\langle (\partial v / \partial t)^2 \rangle^{1/2}} = 16.6\text{mm}$. The Taylor scale is thus about

85 times the Kolmogorov scale. The Taylor-scale Reynolds number is $Re_\lambda = \frac{v_{rms}\lambda}{\nu} = 2000$. This number is actually not constant along the whole data set and fluctuates by about 20%.

We have checked that the standard scaling laws previously reported in the literature are recovered with this time series. In particular, we have verified the validity of the power-law scaling $E(k) \sim k^{-\beta}$ with an exponent β very close to $\frac{5}{3}$ over a range more than two decades, similar to Fig. 5.4 of [14] provided by Gagne and Marchand on a similar data set from the same experimental group. Similarly, we have checked carefully the determination of the inertial range by combining the scaling ranges of several velocity structure functions (see Fig. 8.6 of [14, Fig. 8.6]). Conservatively, we are led to a well-defined inertial range $60 \leq r/\eta \leq 2000$.

III. SCALING PROPERTIES OF INVERSE STRUCTURE FUNCTIONS

A. The probability distributions of exit distances

We have obtained the exit times for 26 δv values: 0.01, 0.0178, 0.0316, 0.0562, 0.1, 0.2, 0.3, 0.4, 0.5, 0.6, 0.7, 0.8, 0.9, 1, 1.1, 1.2, 1.3, 1.4, 1.5, 1.6, 1.7, 1.8, 1.9, 2, 2.33, and 2.7144 m/s. Fig. 1 shows the probability density functions (pdf's) $P(r)$ as a function of r/σ for different velocity thresholds $\delta v = 0.5\text{m/s}$ (\square), $\delta v = 1\text{m/s}$ ($*$), $\delta v = 1.5\text{m/s}$ (\triangleleft) and $\delta v = 2\text{m/s}$ (\star), where $\sigma^2 = \langle r^2 \rangle$ is a function of δv . It is natural to normalize the exit distances by their standard deviation $\sigma(\delta v)$ for a given δv and obtain the pdf of these normalized exit distances $x = r/\sigma$ as

$$\Phi(x) = \sigma P(x\sigma) . \quad (3)$$

The inset of Fig. 1 plots the corresponding $\Phi(x)$ for the four δv values. One can observe an approximate collapse for $0.1 \leq x \leq 10$ but with increasing deviations for large x 's. This is due to the fact that the pdf's $P(r)$ for large δv in the semi-logarithmic plot exhibit approximate linear behaviors over a broad range of the normalized exit distances (exponential distribution), while small δv 's have their pdf's with fatter tail (stretched exponential distribution). Thus, the pdf's of exit distances are not entirely described by the single scale $\sigma(\delta v)$ but are in addition slowly varying in this structure as a function of δv . We propose to parameterize the shape of the pdf's as

$$\Phi(x) = A \exp[-(x/x_0)^m] , \quad \text{for } x \gtrsim 1 \quad (4)$$

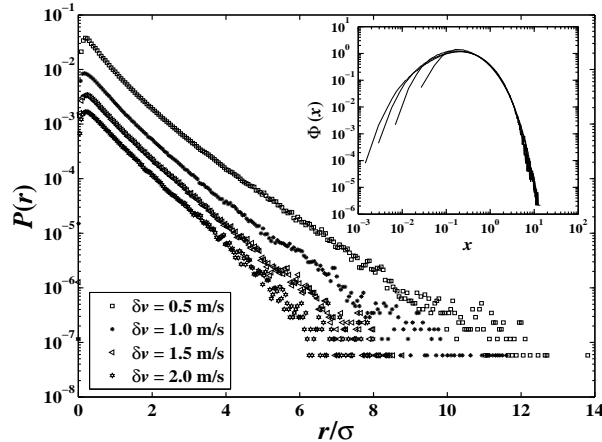


FIG. 1: Empirical probability density function $P(r)$ as a function of normalized exit distance r/σ for $\delta v = 0.5, 1.0, 1.5,$ and 2.0 m/s. The inset shows the dependence of the corresponding $\Phi(x)$ with respect to $x = r/\sigma$ defined by (3).

where the exponent m is a function of δv . This is quite different from the inverse statistics extracted from the time series of financial returns, for which the distributions of exit times have power law tails [15, 16, 17, 18, 19]. Actually, stretched exponential distribution is ubiquitous in natural and social sciences, exhibiting “fat tails” (slower decaying than exponential) with characteristic scales x_0 [20], while power law distributions have fat tails and are scale-free.

Figure 2 presents the fitted exponents m and the characteristic scales x_0 as a function of δv . Two regimes are observed.

- For $\delta v \lesssim 1.5$, the exponent m increases approximately linearly with δv as $m \approx 0.20 \times \delta v + 0.63$.
- For $\delta v \gtrsim 1.5$, m is approximately constant with a value compatible with $m = 1$ corresponding to pure exponential distributions.

B. Convergence of $x^p \Phi(x)$

A preliminary condition for analyzing the inverse structure functions is the accuracy of the moments of exit distances. One necessary condition for T_p defined by (1) to converge

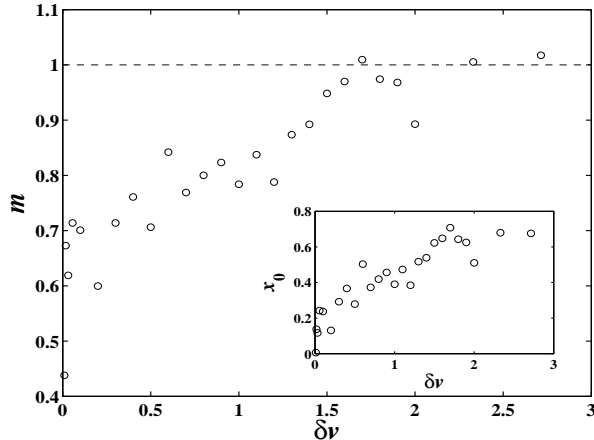


FIG. 2: The dependence of the fitted exponents m and characteristic scales x_0 (inset) with respect to δv .

is that the integrand $r^p P(r)$ or $x^p \Phi(x)$ converges to zero at large r , which requires the closure of the integrand [21]. We have investigated $x^p \Phi(x)$ for different powers p and values $\delta v \in [0.01, 2.7144]$ to determine how noisy is the range of r 's that contribute primarily to $T_p(\delta v)$. Fixing p , $x^p \Phi(x)$ is more noisy for larger δv . For instance, $x^6 \Phi(x)$ clearly converges for $\delta v = 0.5$ m/s, but not for $\delta v = 2.0$ m/s. We find that $T_p(\delta v)$ with p up to 5 can be evaluated with good statistical confidence. For $p = 6$, a reasonably good evaluation of $T_6(\delta v)$ is obtained for small δv . The integrands for $q \geq 8$ seem divergent and the evaluation of the corresponding $T_p(\delta v)$ are less sound statistically. The typical dependence of $x^p \Phi(x)$ as a function of x are shown in Fig. 3 for $\delta v = 1.5$ m/s and $p = 1, 2, 4, 6, 8$ and 10.

We now offer an estimate of the data size needed to estimate reliable inverse structure functions T_p for different orders p . Let us assume that x has a stretched exponential distribution (3) for x greater than some x_0 . Thus, the integrand of T_p is $\mathcal{I}(x) = Ax^p e^{-(x/x_0)^m}$, where is a normalizing constant. We estimate that a reliable estimation of T_p requires a good convergence of the integrand up to a value several times the value x_c for which the integrand achieves its maximum (we use a factor $\kappa \approx 2 - 3$ according to Fig. 3). For the form of the stretched exponential distribution (4), we have $x_c = x_0(p/m)^{1/m}$. On the other hand, the largest typical value x_{\max} observed in a sample of size N is determined by the standard condition

$$N \int_{r_{\max}}^{\infty} \Phi(x) dx \simeq 1, \quad (5)$$

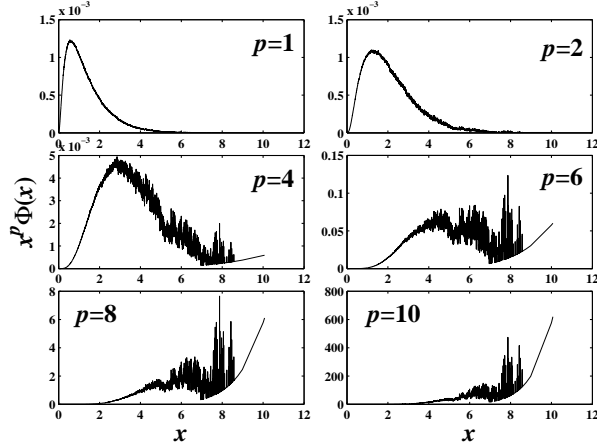


FIG. 3: Plots of $x^p\Phi(x)$ as a function of x for different values of p and velocity threshold $\delta v = 1.5$ m/s.

where the integration can be performed analytically in terms of a Whittaker M function. When $\Phi(x)$ is exponential, expression (5) leads to the simple equation

$$N = (m/A)e^{mx_{\max}} . \quad (6)$$

We now write that $T_p(\delta v)$ is reasonably well-estimated if the range of x extends at least κ times beyond x_c . This amounts to the condition $x_{\max} = \kappa x_c$, where κ is approximately independent of δv . It follows that the minimum sample size necessary to calculate $T_p(\delta v)$ for an exponential distribution of x 's ($m = 1$) is given by

$$N(p) = (m/A)e^{\kappa p} . \quad (7)$$

For $\kappa \simeq 2$ as suggested from the left-middle panels of Fig. 3, with $A \approx 1/x_0$ with $x_0 \approx 0.7$ (see Fig. 2), we find $N(p = 8) \approx 6 \cdot 10^6$ and $N(p = 9) \approx 5 \cdot 10^7$. Thus, our data set with $N \approx 1.7 \times 10^7$ data points should allow us to get a reasonable estimate of the 8th order structure function but higher-orders become unreliable.

C. Extended self-similarity of inverse structure functions

To investigate the scaling properties of the inverse structure functions, we define a set of relative exponents using the framework of extended self-similarity (ESS) [22]:

$$T_p(\delta v) \propto [T_{p_0}(\delta v)]^{\xi(p,p_0)}, \quad (8)$$

where p_0 is a reference order. In the case of velocity structure functions, $p_0 = 3$ is a quite natural choice based on the exact Kolmogorov's four-fifth law. There is no similar reference for the scaling properties of the inverse structure functions and we choose somewhat arbitrarily $p_0 = 2$. In general, ESS provides a wider scaling range for the extraction of scaling exponents. We will see in this subsection that Eq. (8) holds for our experimental data of turbulence with a high accuracy.

Figure 4 presents log-log plots of $T_p(\delta v)$ vs $T_2(\delta v)$ for $p = 1, 2, \dots, 10$ with $\delta v \in [0.01, 2.7144]$. The straight lines hold for $0.2 \leq \delta v \leq 2.7144$ and over at least four orders of magnitudes in $T_2(\delta v)$, showing the existence of extended self-similarity in the inverse structure functions. The scaling range for small p 's seems to be broader than for large p 's.

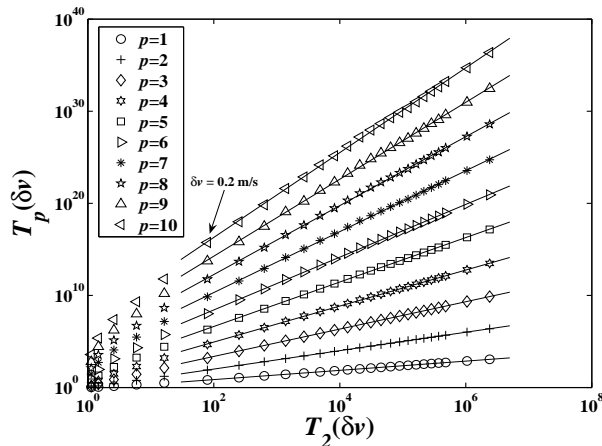


FIG. 4: Dependence of the inverse structure function of order p as a function of the inverse structure function of order 2 taken as a reference. The straight lines exemplify the extended self-similarity of inverse structure functions for the threshold δv ranging from 0.2m/s to 2.7144m/s.

The ESS scaling exponents $\xi(p, 2)$ are shown in Fig. 5. The error bars on $\xi(p, 2)$ corresponds to \pm one standard deviation. There is an indication that $\xi(p, 2)$ has a nonlinear dependence as a function of p , with a downward curvature making the curve depart from the linear dependence $\xi(p, 2) = p/2$ observes for small p 's.

The monoscaling behavior

$$\xi(p, 2) = p/2 \quad (9)$$

is predicted from the assumption that the pdf $\Phi(x)$ of the normalized exit distances, and given by (4), is independent of δv . By definition, we have $T_p(\delta v) = \langle r^p \rangle_{\delta v} = \int_0^\infty r^p P_{\delta v}(r) dr =$

$[\sigma(\delta v)]^p \int_0^\infty dx \Phi_{\delta v}(x) x^p$. Thus,

$$T_p(\delta v) = [T_2(\delta v)]^{p/2} \frac{\int_0^\infty dx \Phi_{\delta v}(x) x^p}{[\int_0^\infty dx \Phi_{\delta v}(x) x^2]^{p/2}}. \quad (10)$$

If $\Phi_{\delta v}(x)$ is universal and independent of δv , then the last term in (10) is a number independent of δv (and thus of $T_2(\delta v)$) and the mono-scaling $\xi(p, 2) = p/2$ follows. Thus, the prediction (9) holds for those velocity thresholds δv satisfying the condition that the pdf of exit distance is universal (independent of δv). This is the analog of the K41 prediction on the standard structure functions. In our present case, there are deviations of the pdf's of exit distances from the exponential law at small δv , that we have proposed to be quantified under the form of stretched exponentials (4) with exponents $m(\delta v)$ being a function of δv as shown in Fig. 2. These deviations from exact self-similarity are weaker than for the direct statistics and are revealed more clearly for the higher orders. We can therefore attribute the deviation of the empirical $\xi(p, 2)$ from the self-similarity (9) at high orders to the non-universality of $\Phi_{\delta v}(x)$ which depends on the velocity levels δv .

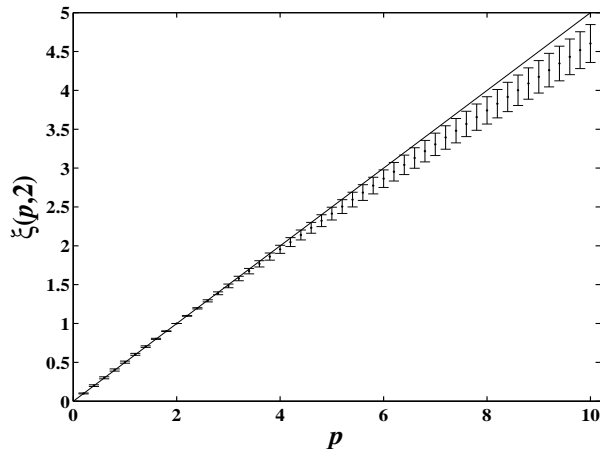


FIG. 5: Dependence of the ESS exponents $\xi(p, 2)$ as a function of the order p of the inverse structure functions. The straight line is the prediction (9) obtained under the assumption of a universal pdf $\Phi_{\delta v}(x)$ of the exit distances (which is independent of the velocity thresholds δv).

IV. MULTIFRACTALITY OF THE TIME SERIES OF EXIT DISTANCES AT DIFFERENT δv

To investigate further the multifractal nature of the exit distance series $\{r(t) : t = 1, \dots, N = 3 \times 11 \times 2^{19} \approx 1.7 \times 10^7\}$ for a given δv , we construct a probability measure μ through its integral function $M(t)$

$$\mu([t_1, t_2]) = M(t_2) - M(t_1) , \quad (11)$$

where $M(t) = 0$ for $0 < t < 1$ and

$$M(t) = \sum_{i=1}^{[t]} r(i) \quad (12)$$

for $1 \leq t \leq N$.

The box-counting method allows us to test for a possible multifractality of the measure μ . The sizes s of the covering boxes are chosen such that the number of boxes of each size is an integer: $n = N/s \in \mathcal{N}$. We construct the partition function Z_q as

$$Z_q(s) \triangleq \sum_{i=1}^n [\mu([i-1)s, is])^q . \quad (13)$$

and expect it to scale as [23, 24]

$$Z_q(s) \sim s^{\tau(q)} , \quad (14)$$

which defines the exponent $\tau(q)$. For $\tau(q)$, a hierarchy of generalized dimensions D_q [25, 26, 27] can be calculated according to

$$D_q = \lim_{p \rightarrow q} \frac{\tau(p)}{p-1} . \quad (15)$$

D_0 is the fractal dimension of the support of the measure. For our measure (11), we have $D_0 = 1$. The local singularity exponent α of the measure μ and its spectrum $f(\alpha)$ are related to $\tau(q)$ through a Legendre transformation [24]

$$\alpha(q) = d\tau(q)/dq , \quad (16a)$$

and

$$f[\alpha(q)] = q\alpha(q) - \tau(q) . \quad (16b)$$

We have tested the power-law scaling of $Z_q(s)$ as a function of the box size s for the exit time sequences at different velocity levels δv . The scaling range is found to span over four orders of magnitude. Figure 6 plots the partition function $Z_q(s)$ for $\delta v = 1.5\text{m/s}$ as a function of the box size s for six different values of q in log-log coordinates. The solid lines are the least-square fits with power laws for each q . The correlation coefficients of the linear regressions (in log-log) are all larger than 0.997, demonstrating the existence of a very good scaling.

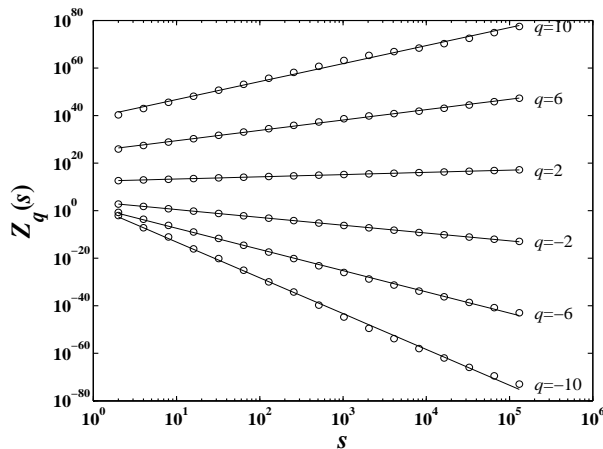


FIG. 6: Plots of $Z_q(s)$ for $\delta v = 1.5\text{m/s}$ as a function of the box size s for different values of q in log-log coordinates. The solid lines are the least-square fits to the data using a linear regression (in log-log coordinates) corresponding to power laws.

The scaling exponents $\tau(q)$ are given by the slopes of the linear fits of $\ln[Z_q(s)]$ as a function of $\ln s$ for different values of δv . Figure 7 plots $\tau(q)$ as a function of q for five different velocity levels δv . The inset shows the fractal spectra $f(\alpha)$ obtained by the Legendre transformation of $\tau(q)$ defined by (16b). We observe that $\tau(q)$'s are concave and nonlinear, a diagnostic of multifractality. The maximal and minimal strength of the set of singularities, α_{\max} and α_{\min} , can be approximated asymptotically by $\lim_{q \rightarrow \infty} D_q = \lim_{q \rightarrow \infty} \tau(q)/q$ and $\lim_{q \rightarrow -\infty} D_q = \lim_{q \rightarrow -\infty} \tau(q)/q$, respectively. It can be clearly observed that the steepness of the curve $\tau(q)$ for negative q increases with δv . Consequently, the maximal singularity α_{\max} increases with δv , as shown in the inset of Fig. 7 where the value of α at the right endpoint increases with δv .

Since μ is conservative, $\tau(1) = 0$ and $\tau(0) = -1$ for all δv . For a given $q < -1$, the function $\tau(q)$ decreases with δv . For a given $q > 1$, there is a critical value δv_c such that

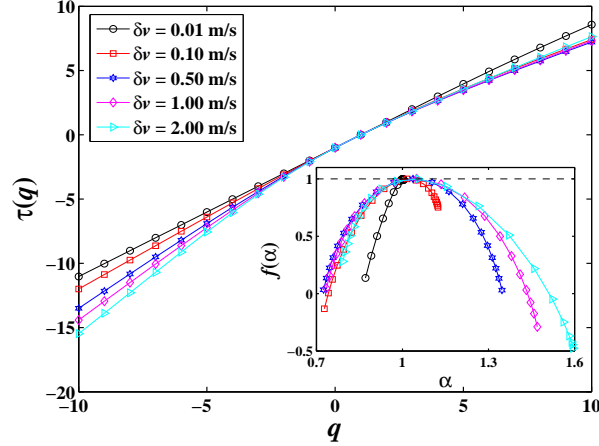


FIG. 7: (Color online) Scaling exponents $\tau(q)$ as a function of q for different velocity levels δv . The inset shows the fractal spectra $f(\alpha)$ obtained by the Legendre transform of $\tau(q)$.

$d\tau(q)/d\delta v < 0$ when $\delta v < \delta v_c$ and $d\tau(q)/d\delta v > 0$ when $\delta v > \delta v_c$. We find that δv_c can be approximated by a linear function

$$\delta v_c = -0.058q + 0.783 , \quad (17)$$

associated with a correlation coefficient of the linear regression equal to 0.963. In addition, one can also see that α_{\min} decreases with δv for $\delta v < \delta v_c$ and increases with δv for $\delta v > \delta v_c$. For $q = -1$, we find for instance that $\delta v_c \approx 1.2\text{m/s}$.

We have performed exactly the same multifractal analysis as done above on synthetic time series generated from a stretched exponential distribution and on reshuffled data of the real exit distances. Both tests give linear scaling exponents $\tau(q) = q - 1$ in a narrower scaling range $64 \leq s \leq 131072$, which is the earmark of monofractality. These tests strengthen the presence of multifractality extracted from the real exit distance data.

In general, multifractality in time series can be attributed to either a hierarchy of changing broad probability density functions for the values of the time series at different scales and/or different long-range temporal correlations of the small and large fluctuations [28]. Our comparison, with reshuffled data and sequences with the same pdf's but no correlation which exhibit trivial monofractality, suggests that multifractality in the set of exit distances may be attributed at least in part to the existence non-trivial dependence in the time series of exit distances.

An important feature of the multifractal spectrum $f(\alpha)$ in the inset of Fig. 7 is the ex-

istence of negative (or latent) dimensions, that is, $f(\alpha) < 0$ [29, 30, 31, 32]. The source of negative dimensions could be twofold. Firstly, the turbulent flow is a stochastic process, which introduces intrinsic randomness in the multifractal measure μ . We note that negative dimensions also appear in continuous multifractals [33, 34, 35]. Secondly, negative dimensions may be interpreted geometrically by considering cuts of higher dimensional multifractals [29, 30, 31]. This intuition proposed by Mandelbrot has been proved mathematically in the multifractal slice theorem [36, 37, 38]. In the present case, the frozen field hypothesis is applied and we deal with one-dimensional cut of the three dimensional turbulence velocity field.

V. CONCLUDING REMARKS

Based on Taylor's frozen field hypothesis, the statistical properties of the exit distances of 3D turbulence have been investigated. The probability density functions of exit distances at different velocity thresholds have been shown to be well approximated by stretched exponentials. The inverse structure functions was shown to exhibit very clear extended self-similarity (ESS). The ESS exponents $\xi(p, 2)$ for small $p < 3.5$ are well described by the monofractal prediction $\xi(p, 2) = p/2$ obtained by assuming a universal exponential distribution of the exit distance. The multifractality is thus related to the dependence of the pdf's of the normalized exit distances on the velocity thresholds δv . We have demonstrated that the sequences of exit distances for each velocity threshold δv exhibit a clear multifractality with negative dimensions. The scaling ranges over which multifractality holds cover more than four order of magnitude in the exit distance variable. The comparison, with reshuffled data and sequences with the same pdf's but no correlation which exhibit trivial monofractality, suggests strongly that our report of multifractality is not artifactual.

Our report of multifractality in the time series of exit distance, which tends to emphasize the least turbulent/most laminar regions, suggests a much richer organization of the weakly turbulent and close to laminar regions than believed until recently.

Acknowledgments

The research by Zhou and Yuan was supported by NSFC/PetroChina jointly through a major project on multiscale methodology (No. 20490200).

- [1] M. H. Jensen, Phys. Rev. Lett. **83**, 76 (1999).
- [2] S. Roux and M. H. Jensen, Phys. Rev. E **69**, 016309 (2004).
- [3] L. Biferale, M. Cencini, A. S. Lanotte, D. Vergni, and A. Vulpiani, Phys. Rev. Lett. **87**, 124501 (2001).
- [4] L. Biferale, M. Cencini, A. S. Lanotte, and D. Vergni, Phys. Fluids **15**, 1012 (2003).
- [5] A. N. Kolmogorov, Dokl. Akad. Nauk SSSR **30**, 9 (1941), (reprinted in Proc. R. Soc.Lond. A **434**, 15-17 (1991)).
- [6] A. N. Kolmogorov, J. Fluid Mech. **13**, 82 (1962).
- [7] B. B. Mandelbrot, in *Lecture Notes in Physics*, edited by M. Rosenblatt and C. van Atta (Springer, 1972), vol. 12, pp. 333–351.
- [8] F. Anselmet, Y. Gagne, E. J. Hopfinger, and R. A. Antonia, J. Fluid Mech. **140**, 63 (1984).
- [9] U. Frisch, A. Mazzino, and M. Vergassola, Phys. Rev. Lett. **80**, 5532 (1998).
- [10] O. Gat, I. Procaccia, and R. Zeitak, Phys. Rev. Lett. **80**, 5536 (1998).
- [11] L. Biferale, M. Cencini, D. Vergni, and A. Vulpiani, Phys. Rev. E **60**, R6295 (1999).
- [12] U. Frisch and M. Vergassola, Europhys. Lett. **14**, 439 (1991).
- [13] C. Meneveau and K. R. Sreenivasan, J. Fluid Mech. **224**, 429 (1991).
- [14] U. Frisch, *Turbulence: The Legacy of A.N. Kolmogorov* (Cambridge University Press, Cambridge, 1996).
- [15] I. Simonsen, M. H. Jensen, and A. Johansen, Eur. Phys. J. B **27**, 583 (2002).
- [16] M. H. Jensen, A. Johansen, and I. Simonsen, Physica A **324**, 338 (2003).
- [17] M. H. Jensen, A. Johansen, and I. Simonsen, Int. J. Mod. Phys. B **17**, 4003 (2003).
- [18] M. H. Jensen, A. Johansen, F. Petroni, and I. Simonsen, Physica A **340**, 678 (2004).
- [19] W.-X. Zhou and W.-K. Yuan (2004), preprint at cond-mat/0410225.
- [20] J. Laherrere and D. Sornette, Eur. Phys. J. B **2**, 525 (1998).
- [21] V. S. L’vov, E. Podivilov, A. Pomyalov, I. Procaccia, and D. Vandembroucq, Phys. Rev. E

- 58**, 1811 (1998).
- [22] R. Benzi, S. Ciliberto, R. Tripiccone, C. Baudet, F. Massaioli, and S. Succi, Phys. Rev. E **48**, R29 (1993).
- [23] U. Frisch and G. Parisi, in *Turbulence and Predictability in Geophysical Fluid Dynamics*, edited by P. G. Gil M, Benzi R (North-Holland, 1985), pp. 84–88.
- [24] T. C. Halsey, M. H. Jensen, L. P. Kadanoff, I. Procaccia, and B. I. Shraiman, Phys. Rev. A **33**, 1141 (1986).
- [25] P. Grassberger, Phys. Lett. A **97**, 227 (1983).
- [26] H. G. E. Hentschel and I. Procaccia, Physica D **8**, 435 (1983).
- [27] P. Grassberger and I. Procaccia, Physica D **9**, 189 (1983).
- [28] J. W. Kantelhardt, S. A. Zschiegner, E. Koscielny-Bunde, S. Havlin, A. Bunde, and H. E. Stanley, Physica A **316**, 87 (2002).
- [29] B. B. Mandelbrot, in *Fractals' Physical Origin and Properties*, edited by L. Pietronero (Plenum, New York, 1989), pp. 3–29.
- [30] B. B. Mandelbrot, Physica A **163**, 306 (1990).
- [31] B. B. Mandelbrot, Proc. Roy. Soc. London A **434**, 79 (1991).
- [32] A. B. Chhabra and K. R. Sreenivasan, PRA **43**, 1114 (1991).
- [33] W.-X. Zhou, H.-F. Liu, and Z.-H. Yu, Fractals **9**, 317 (2001).
- [34] W.-X. Zhou and Z.-H. Yu, Physica A **294**, 273 (2001).
- [35] W.-X. Zhou and Z.-H. Yu, Phys. Rev. E **63**, 016302 (2001).
- [36] L. Olsen, Periodica Mathematica Hungaria **37**, 81 (1998).
- [37] L. Olsen, Hiroshima Math. J. **29**, 435 (1999).
- [38] L. Olsen, Progress in Probability **46**, 3 (2000).